Inorg. Chem. **2008**, *47*, 2764−2776

Bi-, Tetra-, and Hexanuclear Au^I and Binuclear Ag^I Complexes and Ag^I Coordination Polymers Containing Phenylaminobis(phosphonite), $PhN\{P(OC_6H_4OMe\text{-}o)_2\}_2$, and Pyridyl Ligands

Chelladurai Ganesamoorthy,[†] Maravanji S. Balakrishna,*[,†] Joel T. Mague,[‡] and Heikki M. Tuononen[§]

Phosphorus Laboratory, Department of Chemistry, Indian Institute of Technology, Bombay, Powai, Mumbai 400 076, India, Department of Chemistry, Tulane University, New Orleans, Lousiana 70118, and Department of Chemistry, University of Jyväskylä, P.O. Box 35, Jyväskylä, FI-40014, Finland

Received October 30, 2007

The reactions of phenylaminobis(phosphonite), $PhN\{P(OC_6H_4OMe\text{-}o)_2\}_2$ (**1**) (PNP), with $[AuCl(SMe_2)]$ in appropriate ratios, afford the bi- and mononuclear complexes, $[(AuCl)_2(\mu\text{-PNP})]$ (**2**) and $[(AuCl)(PNP)]_2$ (**3**) in good yield. Treatment of **2** with 2 equiv of AgX (X = OTf or ClO_4) followed by the addition of **1** or 2,2′-bipyridine affords $[Au_2(\mu\text{-PNP})_2](OTf)_2$ (**4**) and $[Au_2(C_{10}H_8N_2)_2(\mu\text{-PNP})](ClO_4)_2$ (**5**), respectively. Similarly, the macrocycles $[Au_4(C_4H_4N_2)_2(\mu\text{-PNP})_2](ClO_4)_4$ (**6**), $[Au_4(C_{10}H_8N_2)_2(\mu\text{-PNP})_2](ClO_4)_4$ (**7**), and $[Au_6(C_3H_3N_3)_2(\mu\text{-PNP})_3](ClO_4)_6$ (**8**) are obtained by treating **2** with pyrazine, 4,4′-bipyridine, or 1,3,5-triazine in the presence of $AgClO_4$. The reaction of **1** with AgOTf in a 1:2 molar ratio produces $[Ag_2(\mu\text{-OTf})_2(\mu\text{-PNP})]$ (**9**). The displacement of triflate ions in **9** by **1** leads to a disubstituted derivative, $[Ag_2(\mu\text{-PNP})_3](OTf)_2$ (**10**). The equimolar reaction of **1** with $AgClO_4$ in THF affords $[Ag_2(C_4H_8O)_2(\mu\text{-PNP})_2](ClO_4)_2$ (**11**). Treatment of **1** with $AgClO_4$ followed by the addition of 2,2′-bipyridine affords a discrete binuclear complex, $[Ag_2(C_{10}H_8N_2)_2(\mu\text{-PNP})](ClO_4)_2$ (**12**), whereas similar reactions with 4,4′-bipyridine or pyrazine produce one-dimensional zigzag Ag^I coordination polymers, $[Ag_2(C_{10}H_8N_2)(\mu\text{-}ClO_4)(ClO_4)(\mu\text{-PNP})]_n$ (**13**) and $[Ag_2(C_4H_4N_2)(\mu\text{-}ClO_4)(ClO_4)(\mu\text{-PNP})]_n$ (**14**) in good yield. The nature of metal−metal interactions in compounds **2**, **4**, **5**, and **12** was analyzed theoretically by performing HF and CC calculations. The structures of the complexes **2**, **4**, **5**, **7**, **9**, **12**, and **14** are confirmed by single crystal X-ray diffraction studies.

Introduction

For the past few decades there has been continued interest in the chemistry of d^{10} metal systems because of their rich photochemical properties,[1] catalytic applications,[2] and use in drug discovery.[3] In addition to a variety of coordination geometries, the short metal−metal contacts, described as "metallophilicity", have been employed in the construction of several macrocyclic molecules and supramolecular architectures via intra- and intermolecular aggregations.[4] The term "aurophilicity" has been introduced to describe the Au^I−Au^I bonding interactions which are comparable in energy with hydrogen bonding.[5] The similar argentophilic and cuprophilic interactions of Ag^I and Cu^I are weaker, and theoretical studies by O'Grady and Kaltsoyannis showed that the strength of the metallophilicity decreases in the order $Au^I > Ag^I > Cu^I$.[6] Although there is ample support for the existence of aurophilicity, examples of metal−metal interactions unsup-

* To whom correspondence should be addressed. Tel.: +91 22 2576 7181. Fax: +91 22 2576 7152/2572 3480. E-mail: krishna@chem.iitb.ac.in.
† Indian Institute of Technology.
‡ Tulane University.
§ University of Jyväskylä.

(1) (a) Vogler, A.; Kunkely, H. *Coord. Chem. Rev.* **2001**, *219*(221), 489–507. (b) Yam, V. W-W.; Chan, C.-L.; Li, C.-K.; Wong, K. M.-C. *Coord. Chem. Rev.* **2001**, *216*(217), 173–194. (c) Yam, V. W.-W.; Lo, K. K.-W. *Chem. Soc. Rev.* **1999**, *28*, 323–334. (d) Henary, M.; Wootton, J. L.; Khan, S. I.; Zink, J. I. *Inorg. Chem.* **1997**, *36*, 796–801. (e) Jansen, M. *Angew. Chem., Int. Ed. Engl.* **1987**, *26*, 1098–1110.

(2) (a) Corti, C. W.; Holliday, R. J. *Gold Bull.* **2004**, *37*, 20–26. (b) Gorin, D. J.; Toste, F. D. *Nature* **2007**, *446*, 395–403. (c) Jimenez-Nunez, E.; Echavarren, A. M. *Chem. Commun.* **2007**, *333*, 346. (d) Hashmi, A. S. K.; Hutchings, G. J. *Angew. Chem., Int. Ed.* **2006**, *45*, 7896–7936. (e) Baker, R. T.; Calabrese, J. C.; Westcott, S. A. *J. Organomet. Chem.* **1995**, *498*, 109–117.

(3) (a) Kolb, H. C.; Sharpless, K. B. *Drug Discovery Today* **2003**, *8*, 1128–1137. (b) Fricker, S. P. *Gold Bull.* **1996**, *29*, 53–60. (c) Mirabelli, C. K.; Hill, D. T.; Faucette, L. F.; McCabe, F. L.; Girard, G. R.; Bryan, D. B.; Sutton, B. M.; Bartus, J. O.; Crooke, S. T.; Johnson, R. K. *J. Med. Chem.* **1987**, *30*, 2181–2190.

10.1021/ic702133f CCC: $40.75
Published on Web 02/13/2008

ported by bridging ligands in Cu^{I} and Ag^{I} systems are exceedingly rare.[7] Fackler and co-workers investigated the importance of this metal−metal interaction in the photophysical properties in a range of Group 11 metal complexes and described the emission energy due to metallophilicity as a function of both metal−metal interactions and the nature of the ligands.[8]

In recent years, several strategies have been developed for the construction of highly soluble polynuclear d^{10} metal complexes using bi- or tridentate phosphorus based ligands.[9] In particular, special emphasis has been focused on the use of bis(diphenylphosphino)methane (dppm) with chalcogenides.[10] Although the transition metal chemistry of the analogous short-bite aminobis(phosphine) ligand system, $X_2PN(R)PX_2$, has been extensively studied,[11] comparatively little work has been reported on the use of these systems in the synthesis of macromolecules and metallapolymers with or without the assistance of other ligands such as pyridyl ligands.[12] Recently, we have reported novel tetranuclear macrocycles and coordination polymers formed by the interaction of the "short-bite" aminobis(phosphonite), PhN(P(OC$_6$H$_4$OMe-*o*)$_2$)$_2$ (PNP) (**1**), with Cu^{I} halides in the presence of bipyridyl linkers.[13] The coordination behavior of **1** with copper(I) salts was similar to that of the PCP type ligands, but the coordination geometries of the resulting complexes were entirely different. In this context, we wanted to investigate the coordinating behavior of **1** with Ag^{I} and Au^{I} metals as the short bite of the ligand can induce effective metal−metal interactions. Further, the presence of pyridyl ligands can alter the electronic properties as well. As a part of our interest[14] and that of others[15] in the transition metal chemistry of cyclic and acyclic diphosphazane ligands, we describe in this paper the first examples of mixed-ligand Au^{I} and Ag^{I} complexes containing the "short-bite" aminobis(phosphonite), PhN(P(OC$_6$H$_4$OMe-*o*)$_2$)$_2$ (PNP) (**1**), and N-hetero aromatic amines. This includes the formation of novel tetra- and hexanuclear Au^{I} macrocycles and Ag^{I} coordination polymers. The crystal and molecular structures of several bi- and tetranuclear complexes including a novel Ag^{I} coordination polymer are also described.

Scheme 1

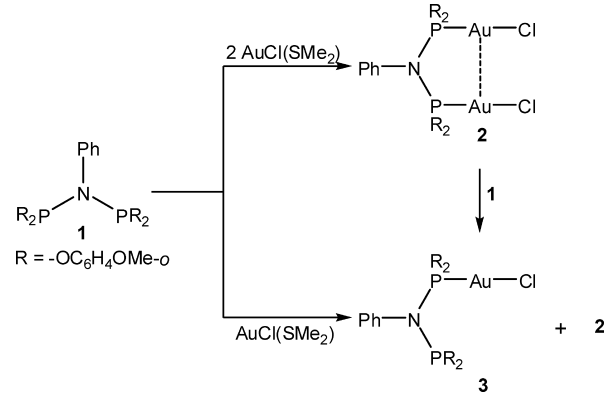

Results and Discussion

Au^{I} Chloride Derivatives. The reaction of the aminobis(phosphonite), PhN(P(OC$_6$H$_4$OMe-*o*)$_2$)$_2$ (hereafter referred as PNP) (**1**), with [AuCl(SMe$_2$)] in a 1:2 molar ratio leads to the formation of a binuclear complex, [(AuCl)$_2$(μ-PNP)] (**2**), with the ligand exhibiting the bridging mode of coordination. A similar reaction in equimolar ratio furnishes a mono-coordinated complex, [(AuCl)(PNP)] (**3**), along with a small quantity of **2**. Treatment of complex **2** with **1** in an equimolar ratio also produces **3** in quantitative yield as shown in Scheme 1. The ^{31}P NMR spectrum of **2** consists of a single

(4) (a) Hunks, W. J.; Jennings, M. C.; Puddephatt, R. J. *Inorg. Chem.* **2002**, *41*, 4590–4598. (b) Schmidbaur, H. *Nature* **2001**, *413*, 31–32. (c) Puddephatt, R. J. *Coord. Chem. Rev.* **2001**, *216*(217), 313–332. (d) Gimeno, M. C.; Laguna, A. *Chem. Rev.* **1997**, *97*, 511–522. (e) Schmidbaur, H. *Chem. Soc. Rev.* **1995**, *24*, 391–400.

(5) (a) Schmidbaur, H. *Gold Bull.* **2000**, *33*, 3–10. (b) Pyykkö, P.; Mendizabal, F. *Inorg. Chem.* **1998**, *37*, 3018–3025. (c) Pyykkö, P. *Chem. Rev.* **1997**, *97*, 597–636.

(6) O'Grady, E.; Kaltsoyannis, N. *Phys. Chem. Chem. Phys.* **2004**, *6*, 680–687.

(7) (a) Zhang, J.-P.; Wang, Y.-B.; Huang, X.-C.; Lin, Y.-Y.; Chen, X.-M. *Chem. Eur. J.* **2005**, *11*, 552–561. (b) Hermann, H. L.; Boche, G.; Schwerdtfeger, P. *Chem. Eur. J.* **2001**, *7*, 5333–5342. (c) Che, C.-M.; Tse, M.-C.; Chan, M. C. W.; Cheung, K.-K.; Phillips, D. L.; Leung, K.-H. *J. Am. Chem. Soc.* **2000**, *122*, 2464–2468. (d) Poblet, J. M.; Benard, M. *Chem. Commun.* **1998**, 1179–1180. (e) Singh, K.; Long, J. R.; Stavropoulos, P. *J. Am. Chem. Soc.* **1997**, *119*, 2942–2943. (f) Siemeling, U.; Vorfeld, U.; Neumann, B.; Stammler, H. G. *Chem. Commun.* **1997**, 1723–1724.

(8) (a) Fackler, J. P., Jr *Inorg. Chem.* **2002**, *41*, 6959–6972. (b) Forward, J. M.; Bohmann, D.; Fackler, J. P., Jr.; Staples, R. J. *Inorg. Chem.* **1995**, *34*, 6330–6336. (c) Assefa, Z.; McBurnett, B. G.; Staples, R. J.; Fackler, J. P., Jr.; Assmann, B.; Angermaier, K.; Schmidbaur, H. *Inorg. Chem.* **1995**, *34*, 75–83.

(9) (a) Lin, Y.-Y.; Lai, S.-W.; Che, C.-M.; Fu, W.-F.; Zhou, Z.-Y.; Zhu, N. *Inorg. Chem.* **2005**, *44*, 1511–1524. (b) Wei, Q.-H.; Zhang, L.-Y.; Yin, G.-Q.; Shi, L.-X.; Chen, Z.-N. *Organometallics* **2005**, *24*, 3818–3820. (c) Yip, J. H. K.; Prabhavathy, J. *Angew. Chem., Int. Ed.* **2001**, *40*, 2159–2162. (d) Bardaji, M.; Laguna, A.; Orera, V. M.; Villacampa, M. D. *Inorg. Chem.* **1998**, *37*, 5125–5130. (e) Xiao, H.; Weng, Y.-X.; Wong, W.-T.; Mak, T. C. W.; Che, C.-M. *J. Chem. Soc., Dalton Trans.* **1997**, 221–226. (f) Che, C.-M.; Yip, H.-K.; Li, D.; Peng, S.-M.; Lee, G.-H.; Wang, Y.-M.; Liu, S.-T. *J. Chem. Soc., Chem. Commun.* **1991**, 1615–1617. (g) Yam, V. W.-W.; Lai, T.-F.; Che, C.-M. *J. Chem. Soc., Dalton Trans.* **1990**, 3747–3752.

(10) (a) Yu, S.-Y.; Zhang, Z.-X.; Cheng, E. C.-C.; Li, Y.-Z.; Yam, V. W.-W.; Huang, H.-P.; Zhang, R. *J. Am. Chem. Soc.* **2005**, *127*, 17994–17995. (b) Chen, J.; Mohamed, A. A.; Abdou, H. E.; Bauer, J. A. K.; Fackler, J. P., Jr.; Bruce, A. E.; Bruce, M. R. M. *Chem. Commun.* **2005**, 1575–1577. (c) Fenske, D.; Langetepe, T.; Kappes, M. M.; Hampe, O.; Weis, P. *Angew. Chem., Int. Ed.* **2000**, *39*, 1857–1860. (d) Yam, V. W.-W.; Cheng, E. C.-C.; Cheung, K.-K. *Angew. Chem., Int. Ed.* **1999**, *38*, 197–199. (e) Tzeng, B.-C.; Che, C.-M.; Peng, S.-M. *J. Chem. Soc., Dalton Trans.* **1996**, 1769–1770.

(11) Balarishna, M. S.; Reddy, S. V.; Krishnamurthy, S. S.; Nixon, J. F.; St. Laurent, J. C. T. R. B. *Coord. Chem. Rev.* **1994**, *129*, 1–90.

(12) (a) Yam, V. W.-W.; Cheng, E. C.-C.; Zhu, N. *Angew. Chem., Int. Ed.* **2001**, *40*, 1763–1765. (b) Yam, V. W.-W.; Cheng, E. C.-C.; Zhou, Z.-Y. *Angew. Chem., Int. Ed.* **2000**, *39*, 1683–1685.

(13) Ganesamoorthy, C.; Balakrishna, M. S.; George, P. P.; Mague, J. T. *Inorg. Chem.* **2007**, *46*, 848–858.

(14) (a) Venkateswaran, R.; Mague, J. T.; Balakrishna, M. S. *Inorg. Chem.* **2007**, *46*, 809–817. (b) Punji, B.; Mague, J. T.; Balakrishna, M. S. *Inorg. Chem.* **2006**, *45*, 9454–9464. (c) Chandrasekaran, P.; Mague, J. T.; Balakrishna, M. S. *Organometallics* **2005**, *24*, 3780–3783. (d) Chandrasekaran, P.; Mague, J. T.; Balakrishna, M. S. *Inorg. Chem.* **2005**, *44*, 7925–7932. (e) Balakrishna, M. S.; George, P. P.; Mague, J. T. *J. Organomet. Chem.* **2004**, *689*, 3388–3394. (f) Punji, B.; Mague, J. T.; Balakrishna, M. S. *Inorg. Chem.* **2007**, *46*, 10268–10275. (g) Balakrishna, M. S.; Mague, J. T. *Organometallics* **2007**, *26*, 4677–4679.

(15) (a) Krishna, H.; Krishnamurthy, S. S.; Nethaji, M. *Polyhedron* **2006**, *25*, 3189–3200. (b) Ganesan, M.; Krishnamurthy, S. S.; Nethaji, M. *J. Organomet. Chem.* **2005**, *690*, 1080–1091. (c) Veige, A. S.; Gray, T. G.; Nocera, D. G. *Inorg. Chem.* **2005**, *44*, 17–26. (d) Ly, T. Q.; Woollins, J. D. *Coord. Chem. Rev.* **1998**, *176*, 451–481.

Scheme 2

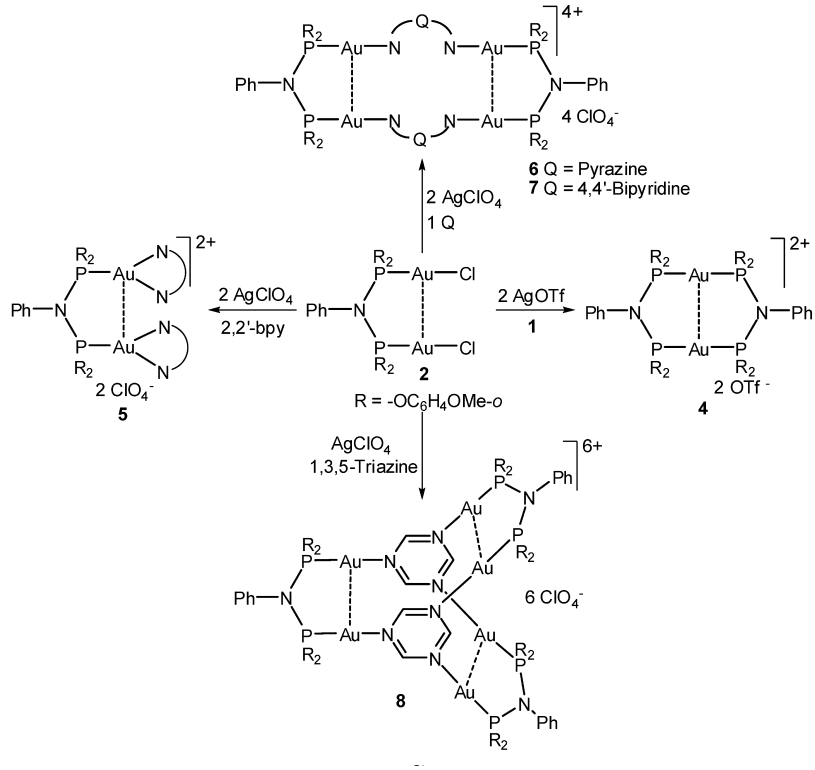

peak at 114.3 ppm whereas **3** shows two doublets centered at 112.2 and 133.8 ppm, with a large $^2J_{PP}$ coupling of 341 Hz.[16] The ^{1}H NMR spectra of **2** and **3** show single resonances corresponding to the *ortho*-methoxy groups at 3.82 and 3.71 ppm, respectively. The structure of complex **2** was confirmed by an X-ray structure determination.

Bi-, Tetra-, and Hexanuclear Au^I Macrocycles. Complex **2** is a potential precursor for the preparation of various bi-, tetra-, and hexanuclear gold(I) macrocycles due to the presence of two highly polar Au−Cl bonds. Treatment of complex **2** with silver salts of poorly coordinating anions followed by the addition of bi- or tridentate ligands resulted in the formation of interesting mixed ligand complexes as shown in Scheme 2. The reaction of **2** with 2 equiv of AgOTf followed by the addition of ligand **1** gives the binuclear complex $[Au_2(\mu\text{-PNP})_2](OTf)_2$ (**4**) whereas the similar reaction with $AgClO_4$ and then 2,2′-bipyridine produces the complex $[Au_2(C_{10}H_8N_2)_2(\mu\text{-PNP})_2](ClO_4)_2$ (**5**) in good yield. The ^{31}P NMR spectra of complexes **4** and **5** show single resonances at 121.9 and 112.0 ppm, respectively. The spectral and analytical data support the proposed formulations of complexes **4** and **5**, and their structures were confirmed through single crystal X-ray diffraction studies.

The reactions of **2** with 2 equiv of $AgClO_4$ followed by addition of 1 equiv of pyrazine or 4,4′-bipyridine produce the tetranuclear macrocycles $[Au_4(C_4H_4N_2)_2(\mu\text{-PNP})_2](ClO_4)_4$ (**6**) and $[Au_4(C_{10}H_8N_2)_2(\mu\text{-PNP})_2](ClO_4)_4$ (**7**) in good yield. In both complexes, the binuclear $(\mu\text{-PNP})Au_2$ moieties are bridged by bipyridyl ligands. Extensive investigations by Puddephatt and co-workers on similar systems have shown that a crossover from macrocyclic ring to sinusoidal polymer was observed when the length of the spacer between the two phosphorus atoms increases.[17] However, this is not true in all cases, and the recent report by the same group has shown that ligands of the type $Ph_2P(CH_2)_nPPh_2$ (n = 1, 3, or 5) prefer to form tetranuclear macrocycles instead of polymeric chains.[18] This leads to the conclusion that the steric/electronic effects may not play any role in the formation of a particular complex. Instead, both the macrocyclic and the polymeric complexes could exist in a rapid equilibrium in solution with the least soluble complex preferentially crystallizing or precipitating from the solution. Because there is no report on the formation of a Au^I polymer with R_2PQPR_2 (Q = −NR′ or −CH$_2$) ligands, we believe that the "rigid short-bite" $R_2PN(R')PR_2$ (where R, R′ = alkyl or aryl) ligands with bulky substituents around the phosphorus centers will prefer to form thermodynamically favored ring structures instead of forming the polymers.[19] The analogous hexanuclear species $[Au_6(C_3H_3N_3)_2(\mu\text{-PNP})_3](ClO_4)_6$ (**8**) was

(16) (a) Keat, R.; Manojlovic-Muir, L.; Muir, K. W.; Rycroft, D. S. *J. Chem. Soc., Dalton Trans.* **1981**, 2192–2198. (b) Colquhoun, I. J.; McFarlane, W. *J. Chem. Soc., Dalton Trans.* **1977**, 1674–1679. (c) Cross, R. J.; Green, T. H.; Keat, R. J. *Chem. Soc. Dalton Trans.* **1976**, 1424–1428. (d) Keat, R. *J. Chem. Soc., Dalton Trans.* **1972**, 2189–2192. (e) Rudolph, R. W.; Newmark, R. A. *J. Am. Chem. Soc.* **1970**, *92*, 1195–1199. (f) Nixon, J. F. *J. Chem. Soc. A* **1969**, 1087–1089.

(17) (a) Wheaton, C. A.; Jennings, M. C.; Puddephatt, R. J. *J. Am. Chem. Soc.* **2006**, *128*, 15370–15371. (b) Puddephatt, R. J. *J. Chem. Soc., Chem. Commun.* **1998**, 1055–1062. (c) Irwin, M. J.; Rendina, L. M.; Vittal, J. J.; Puddephatt, R. J. *J. Chem. Soc., Chem. Commun.* **1996**, 1281–1282. (d) Irwin, M. J.; Vittal, J. J.; Yap, G. P. A.; Puddephatt, R. J. *J. Am. Chem. Soc.* **1996**, *118*, 13101–13102.

(18) Brandys, M.-C.; Jennings, M. C.; Puddephatt, R. J. *J. Chem. Soc., Dalton Trans.* **2000**, 4601–4606.

(19) (a) Tang, H.-S.; Zhu, N.; Yam, V. W.-W. *Organometallics* **2007**, *26*, 22–25. (b) Tzeng, B.-C.; Yeh, H.-T.; Wu, Y.-L.; Kuo, J.-H.; Lee, G.-H.; Peng, S.-M. *Inorg. Chem.* **2006**, *45*, 591–598.

Scheme 3

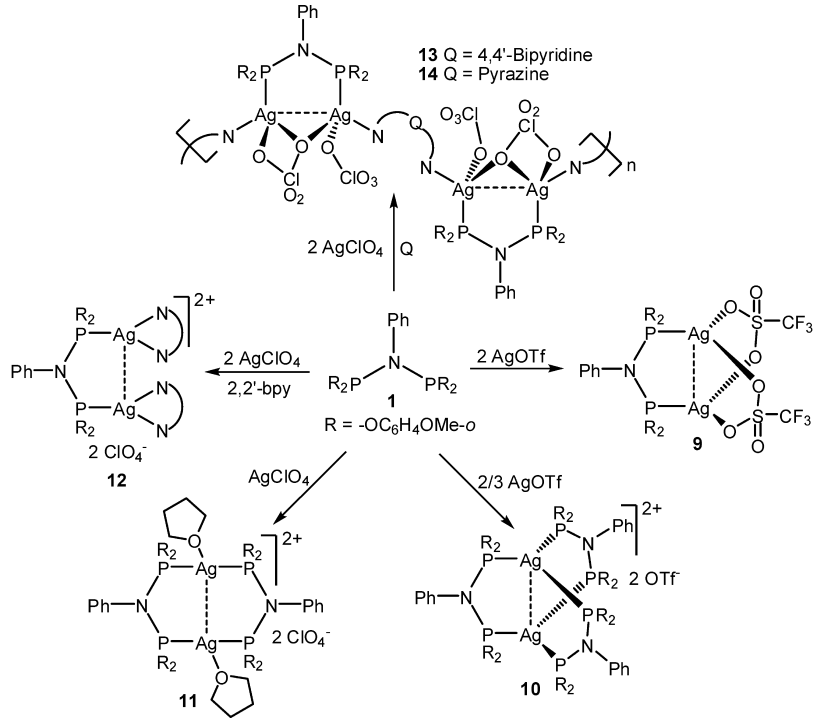

prepared by reacting **2** with $AgClO_4$ and 1,3,5-triazine in a 3:6:2 molar ratio. The ^{31}P NMR spectra of complexes **6**−**8** exhibit single resonances at 117.0, 110.5, and 111.4 ppm, respectively, indicating effective equivalence of all phosphorus atoms. The crystal structure of **7** has been established through a single crystal X-ray diffraction study. Complexes **2**−**8** are colorless, air stable, crystalline solids, highly soluble in CH_2Cl_2, $CHCl_3$, and THF. Although these complexes are moderately stable to air, they turn purple after keeping for a long time even under inert atmosphere.

Silver(I) Derivatives. The reaction of **1** with AgOTf in a 1:2 mole ratio leads to the formation of a binuclear complex, $[Ag_2(\mu\text{-OTf})_2(\mu\text{-PNP})]$ (**9**), in quantitative yield. In complex **9**, the Ag^I atoms are bridged by a pair of trifluoromethanesulfonate ions and a PNP ligand so as to provide trigonal planar geometry around the Ag^I centers. The displacement of trifluoromethanesulfonate ligands in **9** by 2 equiv of **1** afforded a "manxane"-like triply bridged binuclear complex, $[Ag_2(\mu\text{-PNP})_3](OTf)_2$ (**10**), as shown in Scheme 3. The ^{31}P NMR spectrum of complex **9** consists of the A portion of a AA′XX′ multiplet centered at 116.7 ppm, whereas the resonance due to **10** appears at 120.8 ppm as a broad singlet.[20] The complex, $[Ag_2(C_4H_8O)_2(\mu\text{-PNP})_2](ClO_4)_2$ (**11**), has been prepared by reacting an equimolar amount of **1** with $AgClO_4$ in THF. In the ^{31}P NMR spectrum of complex **11**, the resonance appears at 109.2 ppm as a broad doublet due to the complex spin system. In the ^1H NMR spectrum, the resonances corresponding to the coordinated THF molecules appear as two triplets centered at 1.84 and 3.73 ppm with an apparent J_{HH} coupling of 3.6 Hz. The resonance due to the *ortho*-methoxy and aromatic protons appear in the appropriate regions with the expected relative intensities. Although the $^1J_{AgP}$ values for complexes **9**−**11** are significantly larger than that observed in analogous phosphine systems, the expected decrease in $^1J_{AgP}$ values as the number of phosphorus atoms around Ag^I increases from 1 to 3 is consistent with the previous observations in analogous systems.[20] However, low temperature NMR could not be performed because of the poor solubility of the complexes in solvents other than DMSO. The structure of complex **9** was established through a single crystal X-ray diffraction study.

Treatment of **1** with $AgClO_4$ in the presence of 2 equiv of 2,2′-bipyridine produces a binuclear complex, $[Ag_2(C_{10}H_8N_2)_2(\mu\text{-PNP})](ClO_4)_2$ (**12**), whereas the similar reactions with 4,4′-bipyridine or pyrazine afford one-dimensional zigzag Ag^I coordination polymers, $[Ag_2(C_{10}H_8N_2)(\mu\text{-}ClO_4)(ClO_4)(\mu\text{-PNP})]_n$ (**13**) and $[Ag_2(C_4H_4N_2)(\mu\text{-}ClO_4)(ClO_4)(\mu\text{-PNP})]_n$ (**14**), in quantitative yield. The structure of complex **12** is analogous to the Au^I derivative **5** in which the metal centers have trigonal planar geometry being surrounded by a phosphorus atom and a chelating 2,2′-bipyridine ligand. The ^{31}P NMR spectrum of complex **12**, analogous to the spectra observed for the complexes, $[Ag_2(CH_3CN)_2(ClO_4)(\mu\text{-dppm})_2]$[21] and $[AgNO_2(\mu\text{-dppm})]_2$,[22a] consists of a well-resolved A portion of an AA′XX′ multiplet centered at 119.8 ppm with a $[^1J_{AgP}]$ value of 930 Hz. Because of the poor solubility of complex **13** in most suitable solvents, NMR spectroscopic studies could not be carried out, but the molecular composition was confirmed from elemental analysis data. The ^{31}P NMR spectrum of complex **14** shows a broad singlet at 123.5 ppm. The analytical data supports the proposed structures for complexes **12**−**14**, and the structures

(20) (a) Sekabunga, E. J.; Smith, M. L.; Webb, T. R.; Hill, W. E. *Inorg. Chem.* **2002**, *41*, 1205–1214. (b) Muetterties, E. L.; Alegranti, C. W. *J. Am. Chem. Soc.* **1970**, *92*, 4114–4115.

Table 1. NMR Data for Compounds **1**–**14**

compound	$^{31}P\{^{1}H\}$ NMR (in ppm)	^{1}H NMR (in ppm) OCH_3	^{1}H NMR (in ppm) aryl protons
1	132.2 (s)	3.62 (s)	6.76–7.60 (m)
2	114.3 (s)	3.82 (s)	6.82–7.78 (m)
3	133.8 (d) 112.2 (d) $^{2}J_{PP} = 341$ Hz	3.71 (br s)	6.80–7.65 (m)
4	121.9 (s)	3.60 (s)	6.44–7.59 (m)
5	112.0 (s)	3.88 (s)	6.86–8.37 (m)
6	117.0 (br s)	3.92 (s)	6.66–8.70 (m)
7	110.5 (s)	3.85 (s)	6.79–8.52 (m)
8	111.4 (s)	3.76 (s)	6.42–8.80 (m)
9	116.7 (m)	3.88 (s)	6.42–7.70 (m)
10	120.8 (br s)	3.56 (s)	6.78–7.52 (m)
11	109.2 (m)	3.43 (s)	6.76–7.55 (m)
12	119.8 (m) $^{2}J_{PP} = 67$ Hz	3.73 (s)	6.64–8.00 (m)
14	123.5 (br s)	3.74 (s)	6.72–8.47 (m)

of complexes **12** and **14** are confirmed by single crystal X-ray diffraction studies. Although the complexes **9**−**14** are moderately stable to air, they undergo dissociation in solution to give insoluble metallic residues. Full ^{1}H and ^{31}P NMR spectral data for complexes **1**−**12** and **14** are given in Table 1.

Crystal and Molecular Structures of 2, 4, 5, 7, 9, 12, and 14. Perspective views of the molecular structures of compounds **2**, **4**, **5**, **7**, **9**, **12**, and **14** with atom numbering schemes are shown in Figures 1−7, respectively. A full tabulation of intramolecular Au···Au distances and Au−P bond lengths in complexes having the R_2PQPR_2 (Q = −NR′ or $-CH_2$) framework for comparison with the results presented here is given in Table 2, crystal data and the details of the structure determinations in Table 3, and selected bond lengths and bond angles in Tables 4−6. The molecular structure of **2** consists of a discrete [(μ-PNP)$(AuCl)_2$] species having crystallographically imposed twofold rotation symmetry. The Au^{I} center adopts an approximately linear geometry with a P−Au−Cl angle of 173.21(2)°. The P−Au−Cl units are cis-oriented, there are no close nonbonded contacts to the chlorine atoms, and the intramolecular Au···Au distance is 3.124 Å. This is well within the Au···Au distances considered to represent aurophilic interactions. That it indicates an attractive interaction and not just an approach enforced by ligand constraints (the intraligand P···P separation is 2.861(2) Å) is indicated by the fact that the gold atoms are displaced toward each other from the positions they would have occupied were the P−Au−Cl moieties strictly linear. The Au−P and Au−Cl bond distances are 2.206(1) Å and 2.285(1) Å, respectively, while the P−N−P^{i} bond angle is 117.11(17)°.

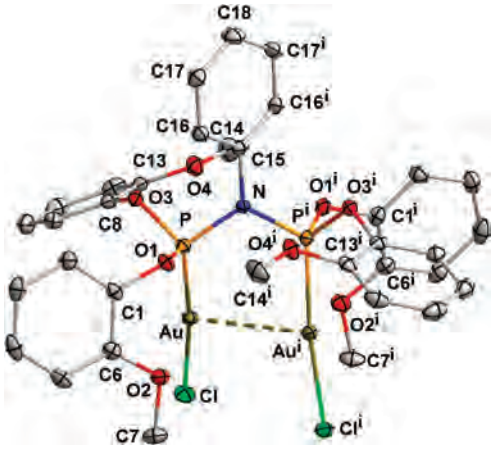

Figure 1. Molecular structure of **2**. All hydrogen atoms have been omitted for clarity. Displacement ellipsoids are drawn at the 50% probability level.

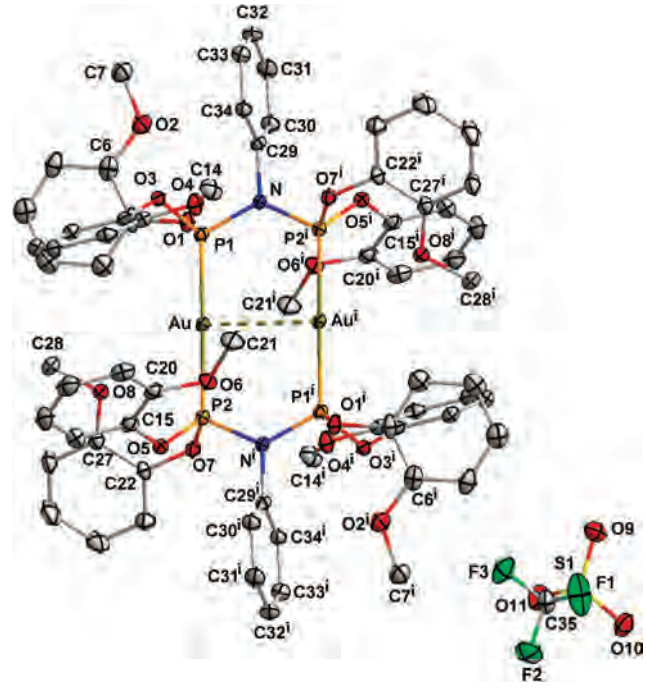

Figure 2. Molecular structure of **4**. All hydrogen atoms and lattice solvents have been omitted for clarity. Displacement ellipsoids are drawn at the 50% probability level.

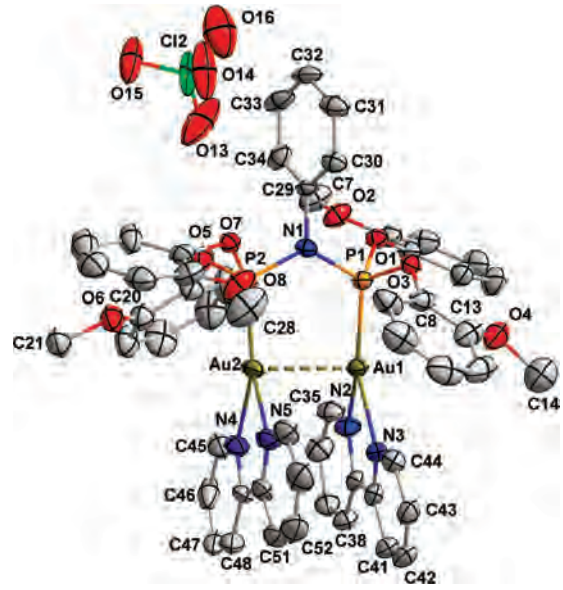

Figure 3. Molecular structure of **5**. All hydrogen atoms, a perchlorate ion, and lattice solvents have been omitted for clarity. Displacement ellipsoids are drawn at the 50% probability level.

The complex **4** consists of a planar eight-membered diauracycle, [−P1−N−P2−Au]$_2$, having crystallographically imposed centrosymmetry. The aminobis(phosphonite) ligands bridge the two metal centers from opposite sides so as to

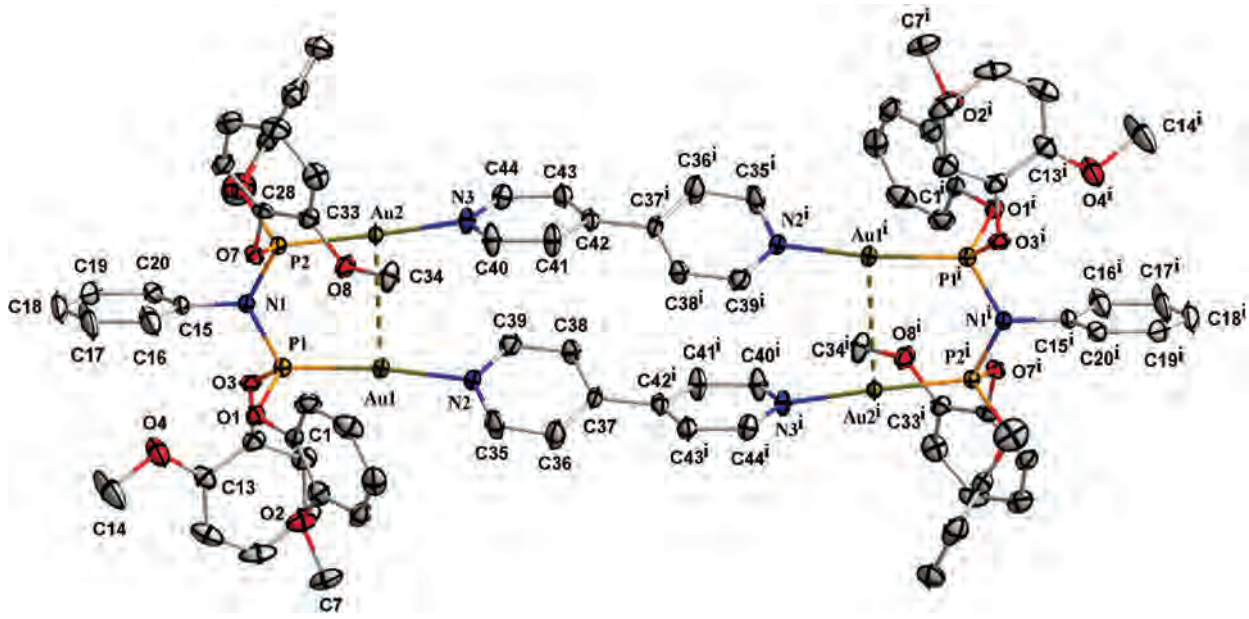

Figure 4. Molecular structure of **7**. All hydrogen atoms and perchlorate ions have been omitted for clarity. Displacement ellipsoids are drawn at the 50% probability level.

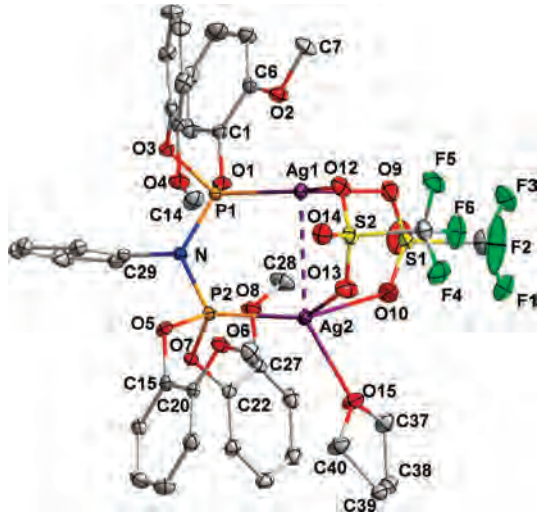

Figure 5. Molecular structure of **9**. All hydrogen atoms have been omitted for clarity. Displacement ellipsoids are drawn at the 50% probability level.

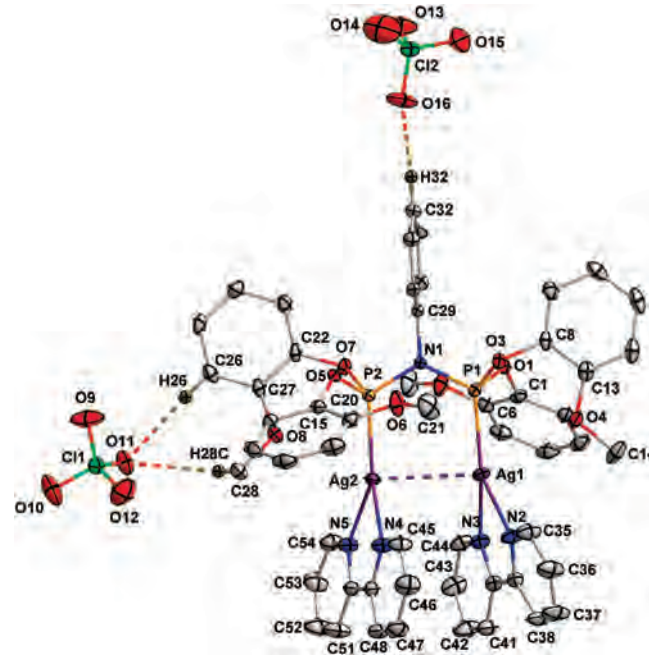

Figure 6. Molecular structure of **12**. All hydrogen atoms and lattice solvents have been omitted for clarity. Displacement ellipsoids are drawn at the 50% probability level.

provide an approximate linear geometry around each Au^I (P1−Au−P2 = 173.50(3)°). This brings the two Au^I centers in close proximity with an intramolecular Au···Au distance of 2.907(1) Å and, as this is shorter than the intraligand P···P separation (2.982(3) Å), an attractive interaction exists. As expected, the P1−Au and P2−Au bond distances (2.292(1) Å and 2.314(1) Å) are longer than those of the corresponding chloro derivative **2** because of the greater trans influence of the phosphonite moiety. The complex has two slightly different P−N bonds with bond distances of 1.662(3) Å and 1.677(3) Å while the P1−N−P2 angle is 126.59(17)° which is larger than that observed in free ligand (116.07(12)°). The trifluoromethanesulfonate ion participates in a number of significant C−H···O and C−H···F hydrogen bonding interactions with neighboring phenyl groups which leads to efficient packing of cations and anions. Specifically, O11 makes contacts of 2.44 Å with H19 (C19−H19···O11 angle = 169°), 2.46 Å with H5 (at $-x$, $2 - y$, $1 - z$; C5−H5···O11 angle = 163°), and 2.67 Å with H12 (C12−H12···O11 angle = 155°). These are comparable to or less than the average C−H···O of 2.62 Å given by Steiner.[22b] In addition, H32 makes a contact of 2.49 Å with F1 (at x, $2.5 - y$, $0.5 + z$; C32−H32···F1 angle = 178°) and H33 contacts F1 (at $-x$, $0.5 + y$, $0.5 - z$; C33−H33···F1 angle = 151°) at 2.58 Å. These can be compared with an average C−H···F distance of 2.60 Å given by Brammer et al.[22c]

In complex **5**, the Au^I atoms have trigonal planar geometry being surrounded by two nitrogen atoms and a phosphorus atom. The sum of the angles around the Au1 and Au2 centers

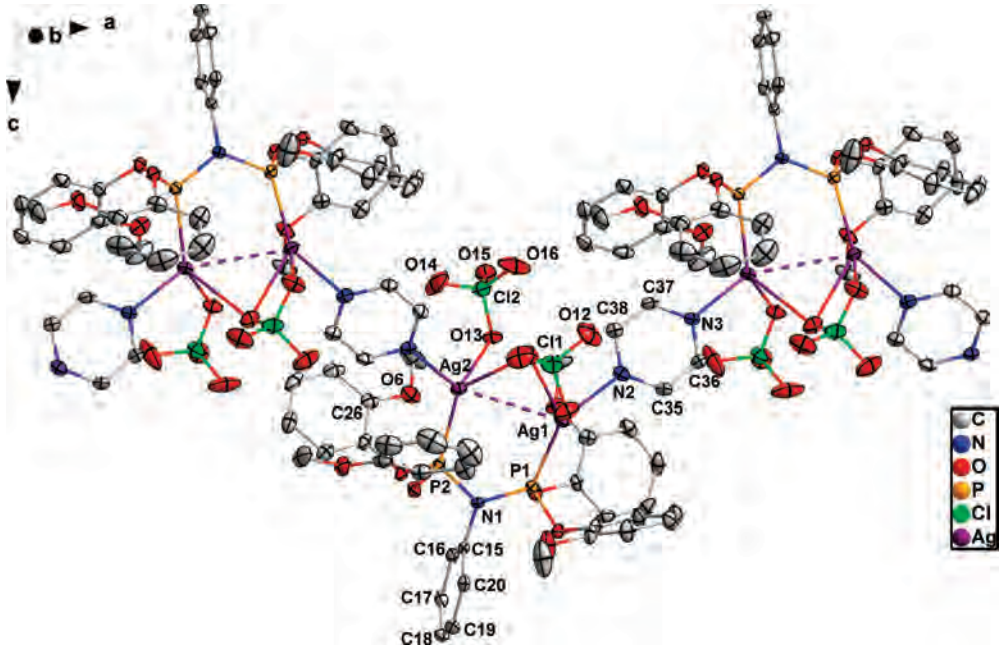

Figure 7. Molecular structure of **14**. All hydrogen atoms have been omitted for clarity. Displacement ellipsoids are drawn at the 50% probability level. View axes: −86.99*X*, −22.32*Y*, − 3.48*Z*. Symmetry operation i = − 0.5 + *x*, *y*, 0.5 − *z*, ii = 0.5 + *x*, *y*, 0.5 − *z*.

Table 2. Au···Au and Au−P Distances[a]

complex	bond distance (Å)		reference
	Au···Au	P−Au	
$[Au_2Cl_2(\mu\text{-dppm})]$	3.351(2)	2.238(1)	26a
$[Au_3Cl_2(\mu\text{-dppm})_2][Au(C_6F_5)_3Cl]$	3.067(5), 3.164(5)	2.322(1)−2.243(1)	26b
$[Au_3Cl_2(\mu\text{-dppm})_2]Cl$	3.076(1)	2.319(3), 2.240(3)	26c
$[\{Au(C_5F_5)\}_2(\mu\text{-dppm})]$	3.163(1)	2.288(3), 2.279(3)	26d
$[m\text{-}(\mu\text{-dppm})Au_2(pzH)_2](ClO_4)_2$	3.133(1)	2.234(5), 2.231(5)	26e
$[Au_2(\mu\text{-dppm})(4,4'\text{-bpy})]_2[CF_3CO_2]_4$	3.106(1), 3.084(1)	2.230(3)−2.241(3)	18
$[(\mu\text{-dppm})Au_2L]_2(ClO_4)_4$	3.148(1)	2.239(2), 2.235(2)	19b
$[\{Au_4(\mu\text{-dppm})_2(C{\equiv}CC_6H_4N)_4]$	3.221(2), 3.131(2)	2.271(1)−2.287(1)	19a
$[\{Au_4(\mu\text{-dcpm})_2(C{\equiv}NC_6H_4N{\equiv}C)_2]$	3.133(3)	2.309(9), 2.313(9)	17c
$[(\mu\text{-dppm})\{Au(2\text{-SPym-4-}NH_2)\}_2]$	3.332(1)	2.261(1), 2.259(1)	27a
$[Au_2(\mu\text{-dppm})\{S_2P(p\text{-}C_6H_4)(OC_5H_9)\}_2]$	3.035(1)	2.259(1), 2.266(2)	27b
$[\{Au(2\text{-}SC_6H_4NH_2)\}_2(\mu\text{-dppm})]$	3.135(1)	2.252(2), 2.250(2)	27c
$[Au_2(\mu\text{-dppm})(TU)]$	2.880(1)	2.235(2), 2.279(2)	27d
$[Au_2(\mu\text{-dppm})(Me\text{-}TU)]$	2.867(1)	2.241(3), 2.279(3)	27d
$[(\mu\text{-dppm})(AuI)_2]$	3.575(1)	2.253(1)	27e
$[(\mu\text{-dppm})Au_2(C_5H_4NS)_2]$	3.048(1)	2.261(1), 2.270(1)	28a
$[(\mu\text{-dppm})\{AuSC(OMe){=}NC_6H_4NO_2\text{-}4\}_2]$	3.159(1)	2.265(1)	28b
$[Au_2(\mu\text{-dmpm})_2](ClO_4)_2$	3.028(2)	2.313(5)	28c
$[Au_2(\mu\text{-dmpm})_2]Br_2$	3.023(1)	2.304(2)	28c
$[Au_2(\mu\text{-dmpm})_2](PF_6)_2$	3.045(1)	2.289(3)	28d
$[Au_2(\mu\text{-dmpm})(\mu\text{-}S_2C_2(CN)_2)]$	2.925(3)	2.268(1), 2.253(1)	28e
$[Au_2(\mu\text{-dcpm})_2][Au(CN)_2]_2$	2.988(1)	2.307(2), 2.316(2)	29a
$[Au_2(\mu\text{-dcpm})_2]Cl_2$	2.992(1)	2.309(1)−2.328(1)	29a
$[Au_2(\mu\text{-dcpm})_2](CO_4)_2$	2.939(1)	2.317(3), 2.320(3)	29a
$[Au_2(\mu\text{-dcpm})_2]I_2$	3.076(1)	2.342(3), 2.321(2)	29a
$[Au_2Cl_2(\mu\text{-}^i Pr_2PCH_2PPh_2)]$	3.418(1)	2.236(1), 2.236(1)	29b
$[Au_2Br_2(\mu\text{-}^i Pr_2PCH_2PPh_2)]$	3.166(1)	2.244(1), 2.240(1)	29b
$[Au_2I_2(\mu\text{-}^i Pr_2PCH_2PPh_2)_2]$	2.993(1)	2.309(2), 2.330(2)	29b
$[\{Au(C_5F_5)\}_2(\mu\text{-}^i Pr_2PCH_2PPh_2)]$	3.093(1)	2.268(2), 2.279(2)	29b
$[Au_2(\mu\text{-}^i Pr_2PCH_2PPh_2)_2](CF_3SO_3)_2$	2.984(1)	2.299(1), 2.302(1)	29b
$[\{\mu\text{-}Ph_2PN(C_6H_{11})PPh_2\}Au_2(SC_6H_4F\text{-}p)_2]$	3.438(1)	2.257(2), 2.267(2)	29c
$[Au_2\{\mu\text{-}Ph_2PN(Et)PPh_2\}_2][SbF_6]_2$	2.838(2)	2.298(5), 2.313(6)	29d
$[Au_3Cl_2\{\mu\text{-}Ph_2PN(Et)PPh_2\}_2]PF_6$	3.037(1)	2.313(2), 2.228(2)	29d
$[\{\mu\text{-}Ph_2PN(^n Pr)PPh_2\}Au_2(C{\equiv}CPh)_2]$	2.840(1)	2.350(3), 2.396(3)	29e
$[\{\mu\text{-}Ph_2PN(^n Pr)PPh_2\}Au_2(C{\equiv}CC_6H_4OMe\text{-}p)_2]$	3.071(1)	2.264(2), 2.271(2)	29e
$[(AuCl)_2(\mu\text{-PNP})]$	3.124(1)	2.206(1)	this work
$[Au_2(\mu\text{-PNP})_2](OTf)_2$	2.907(1)	2.292(1), 2.314(1)	this work
$[Au_2(2,2'\text{-bpy})_2(\mu\text{-PNP})_2](ClO_4)_2$	3.058(1)	2.176(2), 2.168(2)	this work
$[Au_4(4,4'\text{-bpy})_2(\mu\text{-PNP})_2](ClO_4)_4$	3.108(1)	2.216(1), 2.203(1)	this work

[a] dppm = bis(diphenylphosphino)methane; pzH = 3,5-dimethylpyrazole; L = *N*,*N*′-bis-4-methylpyridyl oxalamide; dcpm = bis(dicyclohexylphosphino)methane; 2-SPym-4-NH_2 = 4-amino-2-pyrimidine-thiol; TU = 2-thiouracil; Me-TU = 6-methyl-2-thiouracil; dmpm = bis(dimethylphosphino)methane.

Table 3. Crystallographic Information for Compounds **2**, **4**, **5**, **7**, **9**, **12**, and **14**

	2	**4**	**5**	**7**	**9**	**12**	**14**
empirical formula	$C_{34}H_{33}Au_2Cl_2NO_8P_2$	$C_{72}H_{70}Au_2Cl_4F_6N_2O_{22}P_4S_2$	$C_{55.75}H_{52.50}Au_2Cl_{5.50}N_5O_{16}P_2$	$C_{88}H_{82}Au_4Cl_4N_6O_{32}P_4$	$C_{40}H_{41}Ag_2F_6NO_{15}P_2S_2$	$C_{55}H_{51}Ag_2Cl_4N_5O_{16}P_2$	$C_{38}H_{37}Ag_2Cl_2N_3O_{16}P_2$
fw	1110.39	2153.03	1699.38	2789.16	1231.56	1457.49	1140.29
cryst syst	monoclinic	monoclinic	monoclinic	monoclinic	orthorhombic	monoclinic	orthorhombic
space group	*C*2/*c* (No. 15)	$P2_1/c$ (No. 14)	$P2_1/n$ (No. 14)	$P2_1/n$ (No. 14)	$P2_12_12_1$ (No. 19)	$P2_1/n$ (No. 14)	*Pbca* (No. 61)
a, Å	10.9637(8)	12.638(2)	12.6281(7)	17.779(3)	10.8561(6)	12.950(2)	17.705(1)
b, Å	15.702(1)	13.592(2)	23.964(1)	13.180(2)	17.839(1)	26.116(4)	19.206(1)
c, Å	20.422(1)	23.045(4)	21.555(1)	20.720(3)	23.689(1)	17.448(2)	25.513(1)
β, deg	95.135(1)	99.108(2)	106.233(1)	106.502(2)	90	98.824(2)	90
V, Å^3	3501.6(4)	3908.7(11)	6262.9(5)	4655.3(13)	4587.7(4)	5831.1(14)	8675.5(7)
Z	4	2	4	2	4	4	8
ρ_{calcd}, g cm^{-3}	2.106	1.829	1.802	1.990	1.783	1.660	1.746
μ(Mo Kα), mm^{-1}	8.667	4.111	5.035	6.555	1.108	0.983	1.174
F(000)	2120	2128	3326	2704	2472	2944	4576
crystal size, mm^3	0.08 × 0.11 × 0.17	0.13 × 0.15 × 0.23	0.08 × 0.09 × 0.20	0.05 × 0.12 × 0.13	0.13 × 0.15 × 0.19	0.12 × 0.15 × 0.28	0.05 × 0.09 × 0.15
T (K)	100	100	100	100	100	100	100
2θ range, deg	2.0–28.3	1.6–28.2	2.1–27.5	2.0–28.5	2.1–28.3	2.0–28.3	2.1–26.4
total no. reflns	15466	34027	104087	80872	81837	102474	130027
no. of independent reflns	4218 [R_{int} = 0.020]	9358 [R_{int} = 0.033]	14413 [R_{int} = 0.053]	11656 [R_{int} = 0.058]	11399 [R_{int} = 0.047]	14499 [R_{int} = 0.047]	8905 [R_{int} = 0.101]
GOF (F^2)	1.04	1.04	1.06	1.03	1.04	1.09	1.04
R_1[a]	0.0180	0.0333	0.0411	0.0331	0.0247	0.0419	0.0348
wR_2[b]	0.0434	0.0831	0.1109	0.0774	0.0569	0.1000	0.0724

[a] $R = \sum||F_o| - |F_c||/\sum|F_o|$. [b] $R_w = \{[\sum w(F_o^2 - F_c^2)/\sum w(F_o^2)^2]\}^{1/2}$, $w = 1/[\sigma^2(F_o^2) + (xP)^2]$ where $P = (F_o^2 + 2F_c^2)/3$.

are 358.8° and 359.8°, respectively. The Au1−P1 and the Au2−P2 bond distances (2.1757(15) Å and 2.1677(15) Å) are shorter than those observed in **2** and **3** while the Au−N bond distances vary from 2.235(6) Å to 2.254(6) Å and the bite angles created by the 2,2′-bipyridines at the Au1 and Au2 centers are 72.42(17)° and 73.0(2)°, respectively. Even though the two bipyridyl rings are parallel to each other, there are no significant π-π interactions as a twist of the PAuNN planes about the Au1···Au2 axis by 19.9(1)° makes the two bipyridyl rings to slip away from each other. The perchlorate ion forms a C−H···O hydrogen bond with H33 (H33···O14 = 2.46 Å; C33−H33···O14 angle = 151°) and weaker contacts with other C−H units surrounding it.

The molecular structure of **7** consists of a 26-membered macrocyclic ring containing four gold(I) centers which are bridged by two aminobis(phosphonite) and two 4,4′-bipyridine ligands. The molecule has crystallographically imposed centrosymmetry with the inversion center at the middle of the macrocyclic ring. The geometry about each gold(I) center is approximately linear with P1−Au1−N2 and P2−Au2−N3 bond angles of 173.18(11) and 170.58(10), respectively, and an Au···Au distance of 3.108 Å. As with **2**, there appears to be an attractive Au···Au interaction since the observed Au···Au separation is shorter than the value of approximately 3.29 Å which would be expected for two noninteracting gold atoms placed on the lines directly connecting P1 with N2 and P2 with N3. As the Cl and N-donor ligands have approximately the same trans influence, the P1−Au1 and P2−Au2 bond distances (2.216(1) Å and 2.203(1) Å) are quite similar to those observed in **3** while the P1−N1 and P2−N1 bond distances are 1.671(4) Å and 1.664(4) Å, respectively. The bipyridyl moieties are roughly parallel to one another, and the torsion angle between the two pyridyl rings is 26.8(6)° (C38−C37−C42_a-C41_a). There is a particularly strong C−H···O hydrogen bond between H39 and O13 of one perchlorate ion (H39···O13 = 2.28 Å; C39−H39···O13 angle = 158°) and a weaker one of 2.40 Å between H41 and O9 (at *x*, *y*, −1 + *z*; C41−H41···O9 angle = 164°). There are additional contacts of approximately 2.6 Å which primarily involve phenyl hydrogen atoms surrounding the remainder of the perchlorate ions.

The crystals of **9** suitable for X-ray diffraction analysis were grown by keeping the saturated THF solution of **9** at room temperature for several days (in the dark). The molecular structure consists of two nonequivalent silver ions [trigonal planar (Ag1) and tetrahedral (Ag2) due to THF coordination] bridged by a pair of *cis*-trifluoromethanesulfonate ions and a PNP ligand with an Ag1···Ag2 distance of 3.016(1) Å. This value is longer than those found in the analogous complex [Ag_2(μ-dcpm)(μ-O_2CCF_3)$_2$] (2.889(1) Å)[7c] but shorter than those found in [Ag_2(dppm)$_2$(NO_3)$_2$] (3.085 Å) and [Ag_3(dppm)$_3Br_2$]Br (3.362(3)-3.192(3) Å)[9f] indicating the possibility of a weak metal−metal interaction. However, with three bridging ligands whose distances between donor atoms are all less than the Ag···Ag separation, the latter value may simply be the result of compression of the two metals by the short bites of the bridging ligands. The complex has two slightly different Ag−P bonds

Table 4. Selected Bond Distances and Bond Angles for Complexes **2**, **4**, and **5**

complex **2**				complex **4**				complex **5**			
bond distance (Å)		bond angle (deg)		bond distance (Å)		bond angle (deg)		bond distance (Å)		bond angle (deg)	
P−N	1.676(2)	P−N−P	117.11(2)	P1−N	1.662(3)	P1−N−P2	126.59(2)	P1−N1	1.683(5)	P1−N1−P2	123.9(3)
P−O1	1.600(2)	N−P−Au	117.82(8)	P2−N	1.677(3)	P1−Au−P2	173.50(3)	P2−N1	1.684(5)	P1−Au1−N2	143.14(1)
P−O3	1.598(2)	P−Au−Cl	173.21(2)	P1−Au	2.292(1)	P1−Au−Au	91.13(3)	Au1−P1	2.176(2)	P1−Au1−N3	143.19(1)
P−Au	2.206(1)	Au−P−O1	115.87(7)	P2−Au	2.314(1)	P2−Au−Au	90.47(2)	Au2−P2	2.168(2)	P2−Au2−N4	139.24(2)
Au−Cl	2.285(1)	Au−P−O3	114.65(7)	Au−Au_a	2.907(1)	Au−P1−N	115.81(1)	Au1−N2	2.247(5)	P2−Au2−N5	147.52(2)
Au···Au	3.124(1)			P1−O1	1.595(3)	Au−P2−N	115.38(1)	Au1−N3	2.250(4)	N2−Au1−N3	72.42(2)
				P1−O3	1.588(3)	Au−P1−O1	114.72(1)	Au2−N4	2.254(6)	N4−Au2−N5	73.0(2)
				P2−O5	1.582(3)	Au−P1−O3	116.06(1)	Au2−N5	2.235(6)	Au1−P1−O1	118.22(2)
				P2−O7	1.589(3)	Au−P2−O5	121.86(1)	P1−O1	1.594(4)	Au1−P1−O3	114.71(2)
						Au−P2−O7	112.64(1)	P1−O3	1.614(4)	Au2−P2−O5	115.96(2)
								P2−O5	1.602(4)	Au2−P2−O7	120.31(2)
								P2−O7	1.589(4)	Au1−P1−N1	119.10(2)
								Au1−Au2	3.058(1)	Au2−P2−N1	115.46(2)

Table 5. Selected Bond Distances and Bond Angles for Complexes **7**, **9**, and **12**

complex **7**				complex **9**				complex **12**			
bond distance (Å)		bond angle (deg)		bond distance (Å)		bond angle (deg)		bond distance (Å)		bond angle (deg)	
P1−N1	1.671(4)	P1−N1-P2	123.4(2)	P1−N	1.678(2)	P1−N-P2	121.01(1)	P1−N1	1.672(2)	P1−N1-P2	121.62(1)
P2−N1	1.664(4)	P1−Au1−N2	173.18(1)	P2−N	1.675(2)	P1−Ag1−Ag2	90.04(1)	P2−N1	1.671(2)	P1−Ag1−N2	139.89(6)
Au1−P1	2.216(1)	P2−Au2−N3	170.58(1)	P1−Ag1	2.348(1)	P2−Ag2−Ag1	85.93(1)	Ag1−P1	2.321(1)	P1−Ag1−N3	145.66(6)
Au2−P2	2.203(1)	Au1−P1−N1	118.72(1)	P2−Ag2	2.354(1)	P1−Ag1−O9	123.69(5)	Ag2−P2	2.315(1)	P2−Ag2−N4	143.47(6)
Au1−N2	2.074(4)	Au2−P2−N1	119.21(1)	Ag1−Ag2	3.016(1)	P1−Ag1−O12	145.26(5)	Ag1−N2	2.279(2)	P2−Ag2−N5	141.63(6)
Au2−N3	2.080(4)	Au1−P1−O1	110.02(1)	Ag1−O9	2.359(2)	P2−Ag2−O10	132.85(6)	Ag1−N3	2.268(2)	N2−Ag1−N3	73.04(9)
P1−O1	1.599(3)	Au1−P1−O3	119.63(1)	Ag1−O12	2.247(2)	P2−Ag2−O13	126.67(5)	Ag2−N4	2.261(2)	N4−Ag2−N5	73.08(9)
P1−O3	1.583(3)	Au2−P2−O5	115.37(1)	Ag2−O10	2.362(2)	P2−Ag2−O15	121.94(5)	Ag2−N5	2.279(2)	Ag2−Ag1−P1	88.38(2)
P2−O5	1.589(3)	Au2−P2−O7	113.79(1)	Ag2−O13	2.457(2)	Ag1−P1−N	117.23(7)	P1−O3	1.602(2)	Ag1−Ag2−P2	89.94(2)
P2−O7	1.593(3)			Ag2−O15	2.305(2)	Ag2−P2−N	121.70(7)	P1−O1	1.605(2)	Ag1−P1−O1	110.26(7)
Au1−Au2	3.108(1)			P1−O1	1.614(2)			P2−O5	1.608(2)	Ag1−P1−O3	119.29(8)
				P1−O3	1.604(2)			P2−O7	1.605(2)	Ag2−P2−O5	111.57(7)
				P2−O5	1.622(2)			Ag1−Ag2	2.986(5)	Ag2−P2−O7	120.13(8)
				P2−O7	1.606(2)					Ag1−P1−N1	120.65(8)
										Ag2−P2−N1	119.29(8)

Table 6. Selected Bond Distances and Bond Angles for Complex **14**

bond distance (Å)		bond angle (deg)	
P1−N1	1.675(3)	P1−N1-P2	120.14(2)
P2−N1	1.683(3)	P1−Ag1−N2	138.07(7)
Ag1−P1	2.343(1)	P2−Ag2−N3	116.70(7)
Ag2−P2	2.368(1)	P1−Ag1−O9	118.02(6)
Ag1−N2	2.256(3)	P1−Ag1−O10	134.04(6)
Ag2−N3	2.311(3)	P2−Ag2−O10	131.41(6)
Ag1−O9	2.648(3)	P2−Ag2−O13	125.19(6)
Ag1−O10	2.553(2)	Ag1−P1−N1	123.19(1)
Ag2−O10	2.528(2)	Ag2−P2−N1	121.84(1)
Ag2−O13	2.375(2)	Ag1−O10−Ag2	77.77(7)
Ag1−Ag2	3.189(1)		

Table 7. Optimized Geometrical Parameters (Bond Lengths (Å) and Bond Angles (deg)) for **2**, **4**, **5**, and **12**

compound		*r*(NP)	*r*(PM)	*r*(MM)	∠PNP	∠MPN
2	RHF	1.690	2.285	4.157	126.6	116.9
	CC2	1.702	2.180	2.992	120.6	112.2
4	RHF	1.681	2.406	3.174	131.5	115.6
	CC2	1.687	2.299	2.858	127.9	113.8
5	RHF	1.681	2.450	4.683	129.9	121.1
	CC2	1.687	2.201	2.940	123.2	113.6
12	RHF	1.686	2.607	5.084	128.9	125.7
	CC2	1.689	2.283	3.002	124.2	115.2

(2.348(1) Å and 2.354(1) Å), and the P1−N−P2 bond angle (121.01(11)°) is smaller than that observed in complex **4** (126.59(17)°). The cis arrangement of the triflates seems to be governed by intramolecular contacts. The *o*-methoxyphenoxy groups on P2 are oriented by minimization of contacts with the THF molecule on the same metal such that their methoxy groups are directed toward the center of the molecule. As it is, these generate intramolecular contacts O14···H14a = 2.63 Å, O14···H21b = 2.38 Å, and O11···H28a = 2.56 Å. Considerably shorter contacts would be generated were the triflates in the gauche or trans positions. Also, in the present conformation there is a nice C−H···O hydrogen bond of 2.58 Å between O11 and the C7−H7a unit in the molecule at $^1/_2 + x$, $^1/_2 - y$, $-z$ with an O···H−C angle of 155°.

The structure of **12** is similar to the structure of **5**. However, the Ag1−P1−N1−P2−Ag2 frame is almost planar, and the bipyridyl rings are parallel to each other although they are inclined at an angle of approximately 66° to the above mentioned plane. At approximately 3.9 Å apart there can be no significant $\pi-\pi$ interaction. There are two moderately strong C−H···O hydrogen bonds to the perchlorate ions: C32−H32···O16 (H32···O16 = 2.39 Å; C32−H32···O16 angle = 148°) and C26−H26···O11 (H26···O11 = 2.47 Å; C26−H26···O11 = 170°). The patterns of bond lengths and bond angles in **12** are similar to those observed in complex **6**.

The molecular structure of **14** consist of repeating [(μ-PNP)Ag_2(μ-ClO_4)(ClO_4)] and pyrazine units arranged in an alternating up–down fashion to form a 1D zigzag coordination polymer. The coordination geometry around the silver atom is tetrahedral and consists of one nitrogen atom of the pyrazine, one phosphorus atom of **1**, and two oxygen atoms of perchlorate ions. One of the perchlorate ions coordinates

in a monodentate fashion to Ag2 while the other forms a nearly symmetrical μ-oxo bridge between the two metals as well as forming an unsymmetrical chelate with Ag1. The complex has two different Ag−P bonds with bond distances of 2.343(1) Å and 2.368(1) Å although it is not immediately obvious what is the cause. The Ag1···Ag2 distance is 3.189(1) Å, longer than that observed in complexes **9** and **12**, while the Ag1−N2 and Ag2−N3 bond distances are 2.256(3) Å and 2.311(3) Å, respectively, and the P1−N1−P2 bond angle is 120.14(2).

Theoretical Calculations

Metallophilic attractions such as the argentophilic and aurophilic interactions originate primarily from attractive dispersion forces which overcome the Pauli repulsion between two closed d^{10} shells.[5c] These interactions are rather difficult to quantify computationally as the use of correlated ab initio methods is a prerequisite for theoretical calculations probing metallophilicity. It is generally recognized that the description given by the second order Møllet−Plesset perturbation theory (MP2) somewhat exaggerates the attractive forces,[5b] which, thus, necessitates the use of coupled cluster based approaches to obtain accurate energetics. Although all density functional theory (DFT) based approaches include treatment of electron correlation effects directly built-in to the exchange-correlation functional, they are not suitable for modeling metallophilic interactions because of the fact that most of the modern functionals cannot describe long-range, nonlocal correlation effects dominated by the fluctuating r^{-6} dipole term.[5c,23a] In systems involving heavier elements such as gold, the attractive forces are greatly enhanced by relativistic effects which also need to be taken into account in any theoretical description of metallophilicity.[5c,23b] In practical calculations, this is usually accomplished indirectly by employing relativistically parametrized ECP basis sets for such atoms.

Because the Hartree–Fock (HF) method lacks treatment of dynamic electron correlation, it is unable to account for dispersion-type attractive terms, and the approach unavoidably predicts a repulsive behavior between two metallophilic fragments. Thus, one way to investigate the nature of short-range metal−metal interactions observed experimentally is to compare the results of theoretical calculations carried out at both HF and, for example, coupled cluster (CC) level of theory.[24] Simply put, if the geometrical parameters predicted by the two methods agree with each other as well as with the experimental data, the observed attractive interaction—if it exists—cannot be of the metallophilic type. If, on the other hand, two vastly different interaction distances, one long (HF) and one short (CC), are predicted, the calculations give a good indication of the existence of metallophilic interactions. This method also allows one to estimate the strength of a metallophilic attraction via the difference between the coupled cluster energies of a system at Hartree–Fock and coupled cluster optimized geometries, respectively, divided by the number of metal−metal interactions present.

The nature of metal−metal interactions in compounds **2**, **4**, **5**, and **12** was analyzed theoretically by performing HF and CC calculations. Because correlated ab initio calculations would become extremely time-consuming using a realistic substitution pattern, model structures in which phenyl/methoxyphenyl groups and bipyridine ligands were replaced with hydrogen atoms and diazabutadiene ligands, respectively, were used; in the case of ionic compounds **4**, **5**, and **12** only the structure of the cation was modeled. The predicted metal−metal bond distances as well as other key geometrical parameters are given in Table 7. As expected, the inclusion of electron correlation leads to a significant decrease in phosphorus−metal bond length especially in cations **5** and **12**. The restricted Hartree–Fock method predicts a fully repulsive potential in **2**, **5**, and **12** as metal−metal interaction distances significantly greater than the sum of van der Waals radii are obtained; the Au(I)−Au(I) interaction in the structure **4** is also repulsive though the coordination by two PNP ligands significantly restricts the possible elongation of the metal−metal distance. Conversely, optimization of the systems using the coupled cluster ansatz reveals metallophilic attraction in each case and yields bond parameters in good agreement with the experimental data.

The strength of the metallophilic attraction in systems **2**, **4**, **5**, and **12** can be estimated by calculating the energy difference between the Hartree–Fock and coupled cluster optimized structures at the CC2 level of theory. It should be noted, however, that this procedure gives only a rough (upper) estimate of the true interaction energy. The calculated bond energy is around 45 kJ mol^{-1} for systems **2** and **4** and close to 100 kJ mol^{-1} for the dications in structures **5** and **12**. For the former two species the energy difference is within the typical range (i.e., the energy of a strong hydrogen bond), but the latter two species appear at first sight to be extremely strongly bonded by the metallophilic interaction. However, the calculated interaction energies for **5** and **12** are skewed by intramolecular interactions between the two planar diazabutadiene ligands and significant changes in key geometrical parameters other than the metal−metal distance (see Table 7). Nevertheless, the computational analysis indicates that even in these cases the short Ag(I)−Ag(I) and Au(I)−Au(I) distances are due to metallophilic interaction whose effects to the two structures are clearly seen when electron correlation effects are appropriately treated in calculations.

Conclusion

We have reported the first examples of several bi-, tetra-, and hexanuclear mixed ligand Au^I and Ag^I complexes

(21) Effendy; Di Nicola, C.; Nitiatmodjo, M.; Pettinari, C.; Skelton, B. W.; White, A. H. *Inorg. Chim. Acta* **2005**, *358*, 735–747.
(22) (a) Effendy; Hanna, J. V.; Marchetti, F.; Martini, D.; Pettinari, C.; Pettinari, R.; Skelton, B. W.; White, A. H. *Inorg. Chim. Acta* **2004**, *357*, 1523–1537. (b) Steiner, T. *Cryst. Rev.* **1996**, *6*, 1–57. (c) Brammer, L.; Bruton, E. A.; Sherwood, P. *Cryst. Growth Des.* **2001**, *1*, 277–290.
(23) (a) Pyykkö, P. *Angew. Chem., Int. Ed.* **2002**, *41*, 3573–3578. (b) Pyykkö, P.; Runeberg, N.; Mendizabal, F. *Chem. Eur. J.* **1997**, *3*, 1451–1457.
(24) (a) Mendizabal, F.; Pyykkö, P.; Runeberg, N. *Chem. Phys. Lett.* **2003**, *370*, 733–740. (b) Avramopoulos, A.; Papadopoulos, M. G.; Sadlej, A. J. *Chem. Phys. Lett.* **2003**, *370*, 765–769.

including novel coordination polymers of the aminobis(phosphonite) **1** with various bi- and tridentate pyridyl ligands. Complex **2** readily reacts with rigid bidentate N-donor ligands like 2,2′-bipyridine, 4,4′-bipyridine, and pyrazine in the presence of $AgClO_4$ to give either binuclear or tetranuclear macrocycles depending upon the stoichiometry of the reactants and the reaction conditions. Similar reaction with 1,3,5-triazine produces a hexanuclear complex **8**. The mono-, bi-, and trisubstituted Ag^I derivatives, **9**−**10**, have been prepared by the interaction of **1** with AgX (X = ClO_4 or OTf) in appropriate ratios. The aminobis(phosphonite) **1** reacts with $AgClO_4$ in the presence of 4,4′-bipyridine or pyrazine to give 1D zigzag coordination polymers. The presence of metallophilic interactions in compounds **2**, **4**, **5**, and **12** was analyzed theoretically by performing HF and CC calculations which was also supported by short Ag(I)−Ag(I) and Au(I)−Au(I) distances. Coordination complexes containing coplanar 4,4′-bipyridyl groups often show conducting properties due to the extended conjugation through metal and 4,4′-bipyridyl units. Unfortunately, in the solid state, the structure of the Au^I complex shows it to contain noncoplanar or twisted pyridyl groups which prevent the extension of conjugation. It would be interesting to see whether, with appropriate solvents or anions, it is possible to alter the orientation of the pyridyl groups so that they can switch between coplanar and noncoplanar geometries so as to induce reversible conducting properties. Work in this direction is in progress.

Experimental Section

General Procedures. All manipulations were performed under rigorously anaerobic conditions using Schlenk techniques. The reactions were carried out with minimum exposure to light by wrapping the reaction vessel with aluminum foil. All the solvents were purified by conventional procedures and distilled prior to use.[25] The compounds $PhN\{P(OC_6H_4OMe\text{-}o)_2\}_2$[14e] and $AuCl(SMe_2)$[18] were prepared according to the published procedures. AgX (X = OTf and ClO_4), pyrazine, 1,3,5-triazine, 2,2′-bipyridine, and 4,4′-bipyridine were purchased from Aldrich chemicals and used as such without further purification (*Caution! Perchlorate salts of metal complexes with organic ligands are potentially explosive. A small amount was used in all the reactions and handled with great caution. All perchlorate compounds were tested and found to be resistant to shock*). Other chemicals were obtained from commercial sources and purified prior to use.

Instrumentation. The ^1H and $^{31}P\{^1H\}$ NMR (δ in ppm) spectra were recorded using Varian VXR 300 or VXR 400 spectrometer operating at the appropriate frequencies using TMS and 85% H_3PO_4 as internal and external references, respectively. The microanalyses were performed using a Carlo Erba model 1112 elemental analyzer. The melting points were observed in capillary tubes and are uncorrected.

Synthesis of $[(AuCl)_2\{\mu\text{-}PhN(P(OC_6H_4OMe\text{-}o)_2)_2\}]$ (2). A solution of **1** (0.059 g, 0.092 mmol) in CH_2Cl_2 (5 mL) was added dropwise to a solution of $AuCl(SMe_2)$ (0.054 g, 0.184 mmol) also in CH_2Cl_2 (5 mL). The reaction mixture was allowed to stir at room temperature for 4 h. The resulting solution was concentrated to 3 mL followed by the addition of *n*-hexane to give a white precipitate of **2**. White crystals were obtained upon recrystallization from a 1:1 dichloromethane/*n*-hexane mixture. Yield: 89% (0.09 g). Mp: 200–202 °C (dec). Anal. Calcd for $C_{34}H_{33}Au_2Cl_2NO_8P_2$: C, 36.78; H, 2.99; N, 1.26. Found: C, 36.79; H, 2.96; N, 1.23%. ^1H NMR (400 MHz, $CDCl_3$): δ 3.82 (s, OCH_3, 12H), 6.82–7.78 (m, *Ph*, 21H). $^{31}P\{^1H\}$ NMR (121 MHz, $CDCl_3$): δ 114.3 (s).

Synthesis of $[AuCl\{PhN(P(OC_6H_4OMe\text{-}o)_2)_2\}]$ (3). Method 1. A solution of $AuCl(SMe_2)$ (0.051 g, 0.174 mmol) in CH_2Cl_2 (5 mL) was added dropwise to a stirred solution of **1** (0.112 g, 0.174 mmol) also in CH_2Cl_2 (7 mL). The reaction mixture was allowed to stir at room temperature for 4 h. The resulting solution was concentrated to 3 mL followed by the addition of *n*-hexane to give a white precipitate of **3**. Recrystallization from a 1:1 dichloromethane/*n*-hexane mixture gave **3** as an analytically pure white crystalline substance. Yield: 76% (0.116 g).

Method 2. A solution of **1** (0.055 g, 0.085 mmol) in THF (5 mL) was added dropwise to a solution of **2** (0.094 g, 0.085 mmol) also in THF (8 mL). The reaction mixture was refluxed for 4 h and then cooled to room temperature. The solution was concentrated to 3 mL, layered with 3 mL of *n*-hexane, and kept at −30 °C for one day to give analytically pure white crystals of **3**. Yield: 82% (0.122 g). Mp: 220–222 °C (dec). Anal. Calcd for $C_{34}H_{33}AuClNO_8P_2$: C, 46.52; H, 3.79; N, 1.59. Found: C, 46.56; H, 3.70; N, 1.62%. ^1H NMR (400 MHz, $CDCl_3$): δ 3.71 (br s, OCH_3, 12H), 6.80–7.65 (m, *Ph*, 21H). $^{31}P\{^1H\}$ NMR (162 MHz, $CDCl_3$): δ 133.8 (d, $^2J_{PP}$ = 341 Hz), 112.2 (d).

Synthesis of $[Au_2\{\mu\text{-}PhN(P(OC_6H_4OMe\text{-}o)_2)_2\}_2](OTf)_2$ (4). To a vigorously stirred mixture of **2** (0.077 mg, 0.070 mmol) and AgOTf (0.036 g, 0.140 mmol) in CH_2Cl_2 (7 mL) was added dropwise a solution of **1** (0.045 g, 0.070 mmol) in the same solvent (5 mL) at room temperature. The reaction mixture was stirred at room temperature for 2 h and filtered through celite. The filtrate was concentrated under vacuum, layered with 1 mL of *n*-hexane, and kept at −30 °C to give an analytically pure product of **4** as white crystals. Yield: 72% (0.100 g). Mp: 196–198 °C (dec). Anal.

(25) Armarego, W. L. F.; Perrin, D. D. *Purification of Laboratory Chemicals*, 4th ed.; Butterworth-Heinemann: Linacre House, Jordan Hill, Oxford, U.K., 1996.

(26) (a) Schmidbaur, H.; Wohlleben, A.; Wagner, F.; Orama, O.; Huttner, G. *Chem. Ber.* **1977**, *110*, 1748–1754. (b) Uson, R.; Laguna, A.; Laguna, M.; Fernandez, E.; Villacampa, M. D.; Jones, P. G.; Sheldrick, G. M. *J. Chem. Soc., Dalton Trans.* **1983**, 1679–1685. (c) Lin, I. J. B.; Hwang, J. M.; Feng, D.-F.; Cheng, M. C.; Wang, Y. *Inorg. Chem.* **1994**, *33*, 3467–3472. (d) Jones, P. G.; Thone, C. *Acta Crystallogr.* **1992**, *C48*, 1312–1314. (e) Bachechi, F.; Burini, A.; Galassi, R.; Pietroni, B. R.; Severini, M. *J. Organomet. Chem.* **1999**, *575*, 269–277.

(27) (a) Wilton-Ely, J. D. E. T.; Schier, A.; Mitzel, N. W.; Nogai, S.; Schmidbaur, H. *J. Organomet. Chem.* **2002**, *643*(644), 313–323. (b) Maspero, A.; Kani, I.; Mohamed, A. A.; Omary, M. A.; Staples, R. J.; Fackler, J. P., Jr *Inorg. Chem.* **2003**, *42*, 5311–5319. (c) Bardaji, M.; Calhorda, M. J.; Costa, P. J.; Jones, P. G.; Laguna, A.; Perez, M. R.; Villacampa, M. D. *Inorg. Chem.* **2006**, *45*, 1059–1068. (d) Lee, Y.-A.; Eisenberg, R. *J. Am. Chem. Soc.* **2003**, *125*, 7778–7779. (e) Schneider, D.; Schier, A.; Schmidbaur, H. *Dalton Trans.* **2004**, 1995–2005.

(28) (a) Tzeng, B.-C.; Liao, J.-H.; Lee, G.-H.; Peng, S.-M. *Inorg. Chim. Acta* **2004**, *357*, 1405–1410. (b) Ho, S. Y.; Cheng, E. C.-C.; Tiekink, E. R. T.; Yam, V. W.-W. *Inorg. Chem.* **2006**, *45*, 8165–8174. (c) Jaw, H.-R. C.; Savas, M. M.; Rogers, R. D.; Mason, W. R. *Inorg. Chem.* **1989**, *28*, 1028–1037. (d) Perreault, D.; Drouin, M.; Michel, A.; Miskowski, V. M.; Schaefer, W. P.; Harvey, P. D. *Inorg. Chem.* **1992**, *31*, 695–702. (e) Tang, S. S.; Chang, C.-P.; Lin, I. J. B.; Liou, L.-S.; Wang, J.-C. *Inorg. Chem.* **1997**, *36*, 2294–2300.

(29) (a) Fu, W.-F.; Chan, K.-C.; Cheung, K.-K.; Che, C.-M. *Chem. Eur. J.* **2001**, *7*, 4656–4664. (b) Bardaji, M.; Jones, P. G.; Laguna, A.; Villacampa, M. D.; Villaverde, N. *Dalton Trans.* **2003**, 4529–4536. (c) Yam, V. W.-W.; Chan, C.-L.; Cheung, K.-K. *J. Chem. Soc., Dalton Trans.* **1996**, 4019–4022. (d) Field, J. S.; Grieve, J.; Haines, R. J.; May, N.; Zulu, M. M. *Polyhedron* **1998**, *17*, 3021–3029. (e) Yip, S.-K.; Lam, W. H.; Zhu, N.; Yam, V. W.-W. *Inorg. Chim. Acta* **2006**, *359*, 3639–3648.

Calcd for $C_{70}H_{66}Au_2F_6N_2O_{22}P_4S_2$: C, 42.39; H, 3.35; N, 1.41; S, 3.23. Found: C, 42.43; H, 3.37; N, 1.44; S, 3.25%. ^{1}H NMR (400 MHz, $CDCl_3$): δ 3.60 (s, OCH_3, 24H), 6.44–7.59 (m, *Ph*, 42H). ^{31}P{^{1}H}NMR (121 MHz, $CDCl_3$): δ 121.9 (s).

Synthesis of $[Au_2(C_{10}H_8N_2)_2\{\mu$-PhN$\{P(OC_6H_4OMe$-$o)_2\}_2\}](ClO_4)_2$ (5). A mixture of **2** (0.099 g, 0.089 mmol) and $AgClO_4$ (0.040 g, 0.178 mmol) in CH_2Cl_2 (7 mL) was allowed to stir at room temperature for 2 h. The suspension was filtered through celite into a solution of 2,2′-bipyridine (0.028 g, 0.178 mmol) in the same solvent (2 mL) at room temperature. The resulting reaction mixture was allowed to stir for a further 2 h. The filtrate was concentrated under vacuum, layered with 1 mL of *n*-hexane, and kept at −30 °C to give an analytically pure product of **5** as white crystals. Yield: 81% (0.111 g). Mp: 176–178 °C (dec). Anal. Calcd for $C_{54}H_{49}Au_2Cl_2N_5O_{16}P_2$: C, 41.82; H, 3.18; N, 4.52. Found: C, 41.80; H, 3.18; N, 4.56%. ^{1}H NMR (400 MHz, $CDCl_3$): δ 3.88 (s, OCH_3, 12H), 6.86–8.37 (m, *Ph*, 37H). ^{31}P{^{1}H} NMR (162 MHz, $CDCl_3$): δ 112.0 (s).

Synthesis of $[Au_4(C_4H_4N_2)_2\{\mu$-PhN$\{P(OC_6H_4OMe$-$o)_2\}_2\}_2](ClO_4)_4$ (6). This was synthesized by a procedure similar to that of **5** using **2** (0.185 g, 0.166 mmol), $AgClO_4$ (0.075 g, 0.333 mmol) and pyrazine (0.013 g, 0.166 mmol). An analytically pure white crystalline product of **6** was obtained by keeping the saturated CH_2Cl_2/THF (1:1 mixture) solution of **6** at room temperature for several days. Yield: 64% (0.140 g). Mp: 109–110 °C (dec). Anal. Calcd for $C_{76}H_{74}Au_4Cl_4N_6O_{32}P_4$: C, 34.62; H, 2.83; N, 3.19. Found: C, 34.58; H, 2.80; N, 3.15%. ^{1}H NMR (400 MHz, $CDCl_3$): δ 3.92 (s, OCH_3, 24H), 6.66–8.70 (m, *Ph*, 50H). ^{31}P{^{1}H} NMR (162 MHz, $CDCl_3$): δ 117.0 (br s).

Synthesis of $[Au_4(C_{10}H_8N_2)_2\{\mu$-PhN$\{P(OC_6H_4OMe$-$o)_2\}_2\}_2](ClO_4)_4$ (7). This was synthesized by a procedure similar to that of **5** using **2** (0.084 g, 0.075 mmol), $AgClO_4$ (0.034 g, 0.151 mmol), and 4,4′-bipyridine (0.012 g, 0.075 mmol). Analytically pure white crystals of **7** were obtained by keeping the saturated CH_2Cl_2/*n*-hexane (2:1 mixture) solution of **7** at room temperature for 1 day. Yield: 70% (0.073 g). Mp: 156–158 °C (dec). Anal. Calcd for $C_{88}H_{82}Au_4Cl_4N_6O_{32}P_4$: C, 37.89; H, 2.96; N, 3.01. Found: C, 37.80; H, 2.90; N, 3.06%. ^{1}H NMR (400 MHz, $CDCl_3$): δ 3.85 (s, OCH_3, 24H), 6.79–8.52 (m, *Ph*, 58H). ^{31}P{^{1}H} NMR (162 MHz, $CDCl_3$): δ 110.5 (s).

Synthesis of $[Au_6(C_3H_3N_3)_2\{\mu$-PhN$\{P(OC_6H_4OMe$-$o)_2\}_2\}_3](ClO_4)_6$ (8). This was synthesized by a procedure similar to that of **5** using **2** (0.076 g, 0.069 mmol), $AgClO_4$ (0.031 g, 0.138 mmol), and 1,3,5-triazine (0.004 g, 0.046 mmol). Yield: 48% (0.043 g). Mp: 128–130 °C (dec). Anal. Calcd for $C_{108}H_{105}Au_6Cl_6N_9O_{48}P_6$: C, 33.45; H, 2.73; N, 3.25. Found: C, 33.50; H, 2.79; N, 3.30%. ^{1}H NMR (400 MHz, $CDCl_3$): δ 3.76 (s, OCH_3, 36H), 6.42–8.80 (m, *Ph*, 69H). ^{31}P{^{1}H} NMR (162 MHz, $CDCl_3$): δ 111.4 (s).

Synthesis of $[Ag_2(\mu$-OTf$)_2\{\mu$-PhN$(P(OC_6H_4OMe$-$o)_2)_2\}]$ (9). A solution of **1** (0.068 g, 0.105 mmol) in CH_2Cl_2 (5 mL) was added dropwise to a suspension of AgOTf (0.054 g, 0.210 mmol) also in CH_2Cl_2 (7 mL) with constant stirring. The reaction mixture was allowed to stir at room temperature for 4 h. The resulting solution was concentrated to 4 mL, layered with 2 mL of *n*-hexane and stored at −30 °C for 1 day to afford a white crystalline product. The crystals suitable for X-ray diffraction analysis were grown by keeping the saturated THF solution of **9** at room temperature for several days. Yield: 89% (0.108 g). Mp: 174–176 °C (dec). Anal. Calcd for $C_{36}H_{33}Ag_2F_6NO_{14}P_2S_2$: C, 37.29; H, 2.87; N, 1.21; S, 5.53. Found: C, 37.23; H, 2.85; N, 1.20; S, 5.50%. ^{1}H NMR (400 MHz, $CDCl_3$): δ 3.88 (s, OCH_3, 12H), 6.42–7.70 (m, *Ph*, 21H). ^{31}P{^{1}H} NMR (162 MHz, $CDCl_3$): δ 116.7 (m, $|^1J_{AgP}| = 1026$ Hz).

Synthesis of $[Ag_2\{\mu$-PhN$(P(OC_6H_4OMe$-$o)_2)_2\}_3](OTf)_2$ (10). This was synthesized by a procedure similar to that of **9** using **1** (0.082 g, 0.128 mmol) and AgOTf (0.022 g, 0.085 mmol). Yield: 66% (0.069 g). Mp: 188–190 °C (dec). Anal. Calcd for $C_{104}H_{99}Ag_2F_6N_3O_{30}P_6S_2$: C, 50.97; H, 4.07; N, 1.72; S, 2.62. Found: C, 50.92; H, 4.04; N, 1.69; S, 2.57%. ^{1}H NMR (400 MHz, $CDCl_3$): δ 3.56 (s, OCH_3, 36H), 6.78–7.52 (m, *Ph*, 63H). ^{31}P{^{1}H} NMR (162 MHz, $CDCl_3$): δ 120.8 (br s).

Synthesis of $[Ag_2(C_4H_8O)_2\{\mu$-PhN$(P(OC_6H_4OMe$-$o)_2)_2\}_2](ClO_4)_2$ (11). A solution of **1** (0.057 g, 0.089 mmol) in THF (5 mL) was added dropwise to a suspension of $AgClO_4$ (0.040 g, 0.178 mmol) also in THF (5 mL) with constant stirring. The stirring was continued for 2 h at room temperature, and again a solution of **1** (0.057 g, 0.089 mmol) in THF (5 mL) was added dropwise; the mixture was stirred for a further period of 2 h. The resulting solution was concentrated to 5 mL and stored at room temperature for 24 h to give analytically pure white crystals of **11**. Yield: 89% (0.146 g). Mp: 122–124 °C (dec). Anal. Calcd for $C_{76}H_{82}Ag_2Cl_2N_2O_{26}P_4$: C, 49.34; H, 4.47; N, 1.51. Found: C, 49.30; H, 4.43; N, 1.49%. ^{1}H NMR (400 MHz, $CDCl_3$): δ 1.84 (t, CH_2, 8H), 3.74 (t, OCH_2, 8H), 3.43 (s, OCH_3, 24H), 6.76–7.55 (m, *Ph*, 42H). ^{31}P{^{1}H} NMR (162 MHz, $CDCl_3$): δ 109.2 (m, $|^1J_{AgP}| = 770$ Hz).

Synthesis of $[Ag_2(C_{10}H_8N_2)_2\{\mu$-PhN$(P(OC_6H_4OMe$-$o)_2)_2\}](ClO_4)_2$ (12). A solution of **1** (0.099 g, 0.153 mmol) in CH_2Cl_2 (6 mL) was added dropwise to a suspension of $AgClO_4$ (0.069 g, 0.306 mmol) also in CH_2Cl_2 (8 mL) with constant stirring. The reaction mixture was stirred for 2 h, and then a solution of 2,2′-bipyridine (0.048 g, 0.306 mmol) in CH_2Cl_2 (3 mL) was added dropwise. The resulting solution was concentrated to 4 mL, layered with 2 mL of *n*-hexane, and stored at −30 °C for 3 days to give white crystals of **12**. Yield: 82% (0.172 g). Mp: 150–152 °C (dec). Anal. Calcd for $C_{54}H_{49}Ag_2Cl_2N_5O_{16}P_2$: C, 47.25; H, 3.60; N, 5.10. Found: C, 47.20; H, 3.63; N, 5.15%. ^{1}H NMR (400 MHz, $CDCl_3$): δ 3.73 (s, OCH_3, 12H), 6.64–8.00 (m, *Ph*, 37H). ^{31}P{^{1}H} NMR (162 MHz, $CDCl_3$): δ 119.8 (m, $|^1J_{AgP}| = 930$ Hz, $^2J_{PP} = 67$ Hz).

Synthesis of $[Ag_2(C_{10}H_8N_2)(\mu$-ClO$_4)(ClO_4)\{\mu$-PhN$(P(OC_6H_4OMe$-$o)_2)_2\}]_n$ (13). A solution of 4,4′-bipyridine (0.011 g, 0.070 mmol) in CH_2Cl_2 (3 mL) was added dropwise to a mixture of **1** (0.045 g, 0.070 mmol) and $AgClO_4$ (0.029 g, 0.140 mmol) also in CH_2Cl_2 (5 mL) with constant stirring. The resulting white cloudy precipitate was collected by filtration and washed with diethyl ether twice (5 mL each). Yield: 94% (0.080 g). Mp: 186–188 °C (dec). Anal. Calcd for $C_{44}H_{41}Ag_2Cl_2N_3P_2O_{16}$: C, 43.44; H, 3.40; N, 3.45. Found: C, 43.48; H, 3.43; N, 3.50%.

Synthesis of $[Ag_2(C_4H_4N_2)(\mu$-ClO$_4)(ClO_4)\{\mu$-PhN$(P(OC_6H_4OMe$-$o)_2)_2\}]_n$ (14). 14 was synthesized by a procedure similar to that of **12** using **1** (0.065 g, 0.101 mmol), $AgClO_4$ (0.046 g, 0.202 mmol), and pyrazine (0.008 g, 0.101 mmol). Yield: 79% (0.091 g). Mp: 168–170 °C (dec). Anal. Calcd for $C_{38}H_{37}Ag_2Cl_2N_3O_{16}P_2$: C, 40.02; H, 3.27; N, 3.68. Found: C, 40.07; H, 3.24; N, 3.69%. ^{1}H NMR (400 MHz, DMSO-d_6): δ 3.74 (s, OCH_3, 12H), 6.72–8.47 (m, *Ph*, 25H). ^{31}P{^{1}H} NMR (162 MHz, DMSO-d_6): δ 123.5 (br s).

Computational Details. The molecular structures of model systems of compounds **2**, **4**, **5**, and **12** in which phenyl/methoxyphenyl groups and bipyridine ligands were replaced with hydrogen atoms and diazabutadiene, respectively, were fully optimized at both RHF and RI-CC2 levels of theory.[30] Triple-ξ quality basis sets augmented with two polarization functions (def2-TZVPP) were used for all lighter atoms; for gold and silver nuclei, quasi-relativistic

(30) For a description of the RI-CC2 method, see: Hattig, C.; Weigend, F. *J. Chem. Phys.* **2000**, *113*, 5154–5161.

ECP basis sets of equal valence quality were employed.[31] All calculations were performed with the Turbomole 5.9.1 program package[32] using appropriate point group symmetries and MPI-parallelism.

X-ray Crystallography. A crystal of each of the compounds **2**, **4**, **5**, **7**, **9**, **12**, and **14** suitable for X-ray crystal analysis was mounted in a Cryoloop with a drop of Paratone oil and placed in the cold nitrogen stream of the Kryoflex attachment of the Bruker APEX CCD diffractometer. Full spheres of data were collected using 606 scans in ω (0.3° per scan) at $\omega = 0$, 120, and 240° (for **2** and **4**) or a combination of three sets of 400 scans in ω (0.5° per scan) at $\varphi = 0$, 90, and 180° plus two sets of 800 scans in φ (0.45° per scan) at $\omega = -30$ and 210° (for **5**, **7**, **9** **12**, and **14**) under the control of the SMART software package[33a] (for **2**, **4**, **7**, **9**, and **12**) or the APEX2 program suite[33b] (for **5** and **14**). The raw data were reduced to F^2 values using the SAINT+ software,[34] and global refinements of unit cell parameters using 6680–9939 reflections chosen from the full data sets were performed. Multiple measurements of equivalent reflections provided the basis for empirical absorption corrections as well as corrections for any crystal deterioration during the data collection (SADABS[35]). The structures were solved by direct methods (for **5**, **7**, **9**, **12**, and **14**), or the positions of the heavy atoms were obtained from a sharpened Patterson function (for **2** and **4**). All structures were refined by full-matrix least-squares procedures using the SHELXTL program package.[36] Hydrogen atoms were placed in calculated positions and included as riding contributions with isotropic displacement parameters tied to those of the attached nonhydrogen atoms.

Acknowledgment. We are grateful to the Department of Science and Technology (DST), New Delhi, for funding. C.G. thanks CSIR, New Delhi, for a Senior Research Fellowship (SRF). We also thank SAIF, Mumbai, and Department of Chemistry Instrumentation Facilities, Bombay, for spectral and analytical data, and J.T.M. thanks the Louisiana Board of Regents through Grant LEQSF(2002-03)-ENH-TR-67 for purchase of the CCD diffractometer and the Chemistry Department of Tulane University for support of the X-ray laboratory.

Supporting Information Available: X-ray crystallographic files in CIF format for the structure determinations of **2**, **4**, **5**, **7**, **9**, **12**, and **14**. This material is available free of charge via the Internet at http://pubs.acs.org.

IC702133F

(31) All basis sets were taken from the Turbomole 5.9.1 internal basis set library. For explicit basis set listings, see: ftp://ftp.chemie.uni-karlsruhe.de/pub/basen/ or Weigend, F.; Ahlrichs, R. *Phys. Chem. Chem. Phys.* **2005**, *7*, 3297–3305.

(32) Ahlrichs, R.; Bär, M.; Häser, M.; Horn, H.; Kölmel, C. *Chem. Phys. Lett.* **1989**, *162*, 165–169.

(34) *SAINT+*, versions 6.35A and 7.34A; Bruker-AXS: Madison, WI, 2002, 2006.

(35) Sheldrick, G. M. *SADABS*,version 2.05 and version 2007/2; University of Göttingen: Göttingen, Germany, 2002, 2007.

(36) (a) *SHELXTL*, version 6.10; Bruker-AXS: Madison, WI, 2000. (b) Sheldrick, G. M. *SHELXS97 and SHELXL97*; University of Göttingen: Göttingen, Germany, 1997.